9978 *J. Phys. Chem. A* **1998,** *102,* 9978−9985

Hydration Energies and Entropies for Mg^{2+}, Ca^{2+}, Sr^{2+}, and Ba^{2+} from Gas-Phase Ion−Water Molecule Equilibria Determinations

Michael Peschke, Arthur T. Blades, and Paul Kebarle*

Department of Chemistry, University of Alberta, Edmonton, AB, Canada, T6G 2G2

Received: May 5, 1998; In Final Form: September 9, 1998

The sequential enthalpies $\Delta H^\circ_{n-1,n}$, free energies $\Delta G^\circ_{n-1,n}$, and entropies $\Delta S^\circ_{n-1,n}$ for the hydration reaction $M(H_2O)_{n-1}{}^{2+} + H_2O = M(H_2O)_n{}^{2+}$ were determined in the gas phase for M = Mg, Ca, Sr, Ba. The gas-phase ion hydrates were produced by electrospray, and the hydration equilibria were determined in a reaction chamber attached to a mass spectrometer. The exothermicities of the $(n - 1, n)$ reactions at low n ($n = 1$ to $n = 5$) are very high, and the corresponding equilibria require very high temperatures and could not be determined. For these low n, good theoretical results are available for Mg^{2+} and Ca^{2+} (Siegbahn and co-workers). A combination of the theoretical data with the experimental results (from $n = 6$ to $n = 14$) provides information on the inner and outer hydration shell structure and energetics of the hydrates. Very good agreement is observed between the theoretical and experimental energies where they overlap. For Mg, Ca, and Sr the first six molecules go into the inner shell while the seventh and higher molecules go into the outer shell(s). However, the sequential energies indicate crowding in the inner shell of Mg. Six or seven molecules can be filled in the inner shell of Sr, while for Ba the inner shell number may be as high as 8 or 9. The observed entropy changes are, in general, consistent with the assigned shell structures. In particular, there is a large change of $\Delta S_{n-1,n}$ on transition from the inner ($n = 6$) to the outer ($n = 7$) shell for Mg, Ca, and Sr. The difference between the gas-phase total enthalpies $\Delta H^\circ_{0,14}(Ca^{2+}) - \Delta H^\circ_{0,14}(Mg^{2+})$ is within 3 kcal/mol of the total hydration difference $\Delta H^\circ_h(Ca^{2+}) - \Delta H^\circ_h(Mg^{2+})$ for liquid water. A similar result is obtained also for the hydration free energies. Extension of the determinations to ligands that model bonding and coordination in biocomplexes of Mg^{2+} and Ca^{2+} is discussed.

Introduction

Determination of gas-phase equilibria involving singly charged ions such as the oxonium[1,2] and ammonium ion,[3] the alkali ions,[4,5] and solvent molecules such as H_2O, which provide sequential bond free energies, enthalpies and entropies, was initiated some 30 years ago. These studies provided a wealth of data on ion−solvent and ion−ligand interactions,[6,7] which are of importance not only to gas-phase ion chemistry but also to the condensed phase, since they constitute a bridge between gas phase and solution.[8,9] Extensive theoretical computational work[10,11] and experimental studies such as laser spectroscopy of ion clusters in molecular beams[12] were also stimulated by the above work.

The above studies were limited to singly charged ions, yet doubly and multiply charged ions are also of paramount importance in chemistry and biochemistry. The general method used for singly charged ion clusters such as $M^+(H_2O)_n$ is to generate M^+ in the gas phase in which the ligand molecule vapor is present. The formation of $M^+(H_2O)_n$ then proceeds spontaneously by third-body-dependent ion−solvent molecule association reactions. However, this method in general does not work well for multiply charged ions. Collisions of doubly charged metal ions M^{2+} that have high second ionization energies, such as Mg^{2+}, $IE(Mg^+) = 15.0$ eV, or Ca^{2+}, $IE(Ca^+) = 11.9$ eV, with solvent molecules that have low ionization energies such as H_2O, $IE(H_2O) = 12.6$ eV, result not in formation of $M^{2+}(H_2O)_n$ but in two singly charged ions MOH^+ and H_3O^+, precluding thus the formation of high water content ion hydrates by this method; see, for example, Spears and Fehsenfeld.[13]

Doubly and multiply charged ions exist in solution, but preparation of gas-phase ions such as $Mg(H_2O)_n{}^{2+}$ by ion transfer from solution to the gas phase would not have been considered possible until recently. However, new mass spectrometric research has shown that such transfer is feasible. The best method for such an ion transfer is electrospray, developed by John Fenn and co-workers.[14]

Qualitative studies of $M(H_2O)_n{}^{2+}$ ions produced by electrospray where M^{2+} was Mg^{2+}, Ca^{2+}, Sr^{2+}, Ba^{2+}, Mn^{2+}, Fe^{2+}, Co^{2+}, Ni^{2+}, and Zn^{2+} were reported several years ago.[15] More recently, a reaction chamber was developed with which equilibria involving ions produced by electrospray could be determined at different temperatures.[16] The present work presents the first extensive measurements of the equilibria

$$M(H_2O)_{n-1}{}^{2+} + H_2O = M(H_2O)_n{}^{2+} \qquad (n-1, n) \quad (1)$$

for Mg^{2+}, Ca^{2+}, Sr^{2+}, and Ba^{2+}. The binding enthalpies $\Delta H^\circ_{n,n-1}$ when n is low are very high for these ions and particularly so for Mg^{2+} and Ca^{2+}. Thus, theoretical calculations[17,18] predict $\Delta H^\circ_{1,0}(Mg^{2+}) \approx 82$ kcal/mol and $\Delta H^\circ_{1,0}(Ca^{2+}) \approx 57$ kcal/mol. The corresponding equilibria would require very high temperatures, which are inaccessible with the present apparatus. Only binding enthalpies that are less than 30 kcal/mol are accessible, and therefore our measurements were restricted to $(n - 1, n)$ equilibria from $n = 5$ to $n = 15$. Fortunately, theoretical calculations[17,18] of very good reliability have recently become available for $n = 1$ to $n = 6$ for Mg^{2+} and Ca^{2+}. On the other hand, accurate calculations become very difficult at higher n. A combination of the theoretical results with the present data provides thus a very comprehensive description of the hydration thermochemistry of the alkaline earth ions. The coordinative behavior of Mg^{2+} and Ca^{2+} has

10.1021/jp9821127 CCC: $15.00

become of special interest lately[19−24] mainly because of the importance of these ions in biochemical complexes. The theoretical[18] and present experimental work provide information on the coordination numbers for oxygen ligands. The combined theoretical and experimental data also provide relationships to the total hydration energy of the ions in liquid water. Finally, as will be shown, the present results set the stage for further measurements involving ligands that more closely model the bonding and coordination present in biocomplexes involving Mg^{2+} and Ca^{2+}.

Experimental Section

The equilibrium determinations were performed with the ion-reaction chamber previously described.[16a] Briefly, the ions were produced by electrospray of aqueous solutions of the MCl_2 salts at concentrations of $10^{-4}-10^{-3}$ mol/L at flow rates of less than 0.5 μL/min. The atmospheric air and the ions produced were introduced through a capillary into a forechamber containing 10 Torr N_2 gas. An imposed electric field caused the ions to drift into the reaction chamber, which contained nitrogen gas at 10 Torr and known partial pressures of water vapor, $p(H_2O)$, in the 1−100 mTorr range. The reaction chamber was sampled by letting gas and ions escape through an orifice leading to an evacuated chamber and a triple quadrupole mass spectrometer. A very weak drift field, 6 V/cm, was present in the reaction chamber. The observed ion intensity ratio $I(M(H_2O)_n{}^{2+})/I(M(H_2O)_{n-1}{}^{2+}) = \mathrm{Ip}/\mathrm{Ir}$ remained constant for drift fields below 12 V/cm, confirming the expectation[16a] that ions at such low drift fields have thermal internal energies. The ratio Ip/Ir was determined at several water partial pressures, and plots of Ip/Ir versus $p(H_2O)$ led to straight lines as required by the equilibrium expression

$$\frac{\mathrm{Ip}}{\mathrm{Ir}} = K_{\mathrm{eq}}p(\mathrm{H_2O}) \tag{2}$$

where the assumption is made that the ion intensity ratio is equal to the ion concentration ratio near the sampling orifice in the reaction chamber.

The straight lines obtained when extrapolated to Ip/Ir = 0 did not pass exactly through the origin, as required by eq 2, but were displaced to approximately −0.5 mTorr $p(H_2O)$. This displacement can be attributed to ~0.5 mTorr water vapor, from the evaporated solvent used for the electrospray, entering the reaction chamber. This means that the gas countercurrent devices used to prevent such solvent penetration[16a] are very effective but still do not achieve an absolute “shut-off”. The equilibrium constants obtained from the slope of the straight lines and the water pressure augmented by 0.5 mTorr were used for the van’t Hoff plots given in Figures 1−4. Because the ratios were generally determined for $p(H_2O)$ from 1 to ~50 mTorr, the 0.5 mTorr represents only a minor correction.

The reproducibility of the determinations was examined by doing replicate measurements for $Mg(H_2O)_n{}^{+}$ with the same apparatus after a 4-month interval. Shown below is a comparison of the data obtained from van’t Hoff plots in the first and (second) determination. Replicate measurements for ΔG, ΔH, and ΔS respectively give the following: $n = 8$ and 11.0 (10.8), 18.3 (17.8), 24.3 (23.2); $n = 9$ and 9.6 (9.4), 17.3 (16.8), 25.6 (24.7); $n = 10$ and 8.2 (8.0), 15.8 (15.6), 25.7 (25.4); $n = 11$ and 7.1 (6.9), 14.3 (14.2), 24.2 (24.4); $n = 12$ and 6.3 (6.2), 12.7 (13.0), 21.6 (23.0). These data show that in general the values are reproducible within less than 0.2 kcal/mol for ΔG°, 0.5 kcal/mol for ΔH°, and 1.4 cal/(K mol) for ΔS°. However, these results do not include systematic errors such as errors in the determination of the temperature of the gaseous reactants at equilibrium. These are very difficult to assess. We have chosen the following values as estimates of the actual uncertainty: ΔG° 0.5 kcal/mol; ΔH° 1 kcal/mol; ΔS° 2 cal/(K mol).

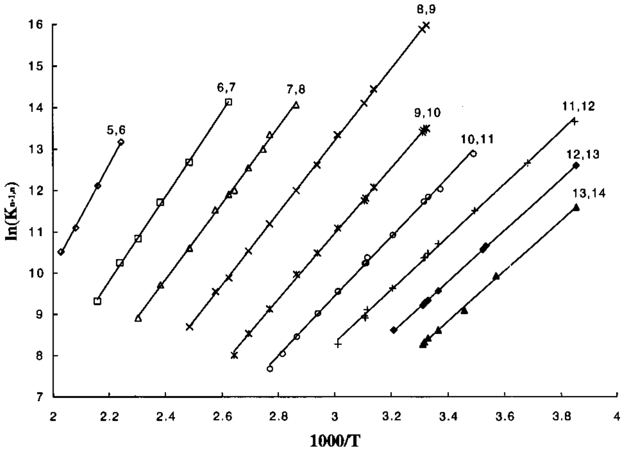

Figure 1. van’t Hoff plots of hydration equilibria of Mg^{2+}: $Mg(H_2O)_{n-1} + H_2O = Mg(H_2O)_n{}^{2+}$.

The high surface tension of water requires a large electrospray onset voltage, and this can lead to electric gas discharges.[16b] In the present experiments, which were with neat water, we used capillary potentials of 3.5−4 kV and suppressed electric discharges by flowing SF_6 gas (40 mL/min) in air (10 L/min) around the electrospray capillary.[16b] In the previous work[15] dealing with doubly charged alkaline earth and transition metal ions M^{2+}, we had used methanol solutions that are easier to electrospray[16b] and exchanged the methanol for water in the reaction chamber, which contained only water vapor. In the present work we found that the use of neat water for the electrospray was advantageous, since the exchange of methanol was not required. Another important advantage was that some ions such as $Be(H_2O)_n{}^{2+}$ and $Cu(H_2O)_n{}^{2+}$, which could not be produced by spray with methanol as solvent,[15] could be obtained with neat water. The fact that these ions could not be produced when methanol was present is in line with the expected more facile charge reduction (see eq 8)[15a] when the higher proton affinity methanol molecule is present. Even though $Be(H_2O)_n{}^{2+}$ with $n = 9, 8, 7$ could be obtained in the present work, determinations of the hydration equilibria of Be^{2+} were found difficult. At the higher reaction chamber temperatures required for the (7, 8) equilibrium, charge reduction leading to the $BeOH(H_2O)_n{}^{+}$ ion was a dominant reaction. This precluded the determination of the (5, 6), (6, 7), and (7, 8) equilibria. Equilibrium constants for $n = 9$ to $n = 14$ could be determined at lower temperatures, and the free energy changes obtained are given in Figure 7.

Results and Discussion

(a) Results from Measurements of the Equilibrium Constants. Plots of the logarithm of the equilibrium constants $K_{n-1,n}$ versus the reciprocal temperature $1/T$ (van’t Hoff plots) for the hydration of Mg^{2+}, Ca^{2+}, Sr^{2+}, and Ba^{2+} are given in Figures 1−4. The enthalpy changes $\Delta H^\circ_{n-1,n}$ obtained from the slopes of the straight lines and the entropy changes obtained from

$$-RT \ln K_{n-1,n} = \Delta G^\circ_{n-1,n} = \Delta H^\circ_{n-1,n} - T\Delta S^\circ_{n-1} \tag{3}$$

are given in Table 1. The free energy changes, $\Delta G^\circ_{n-1,n}$ at $T = 298$ obtained from the straight line plots either by interpolation or by extrapolation to 298 K, are also given in Table 1. The

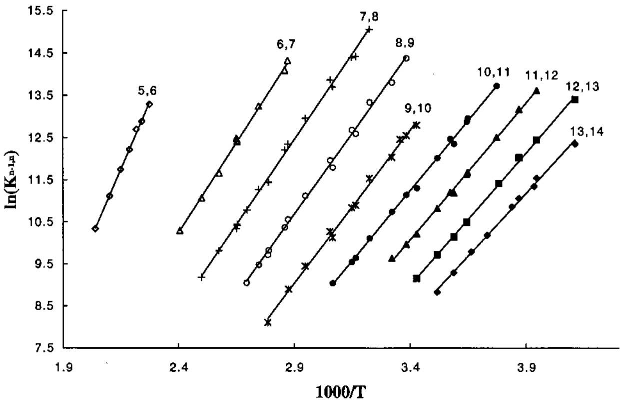

Figure 2. van't Hoff plots of hydration equilibria of Ca^{2+}: $Ca(H_2O)_{n-1}^{2+} + H_2O = Ca(H_2O)_n^{2+}$.

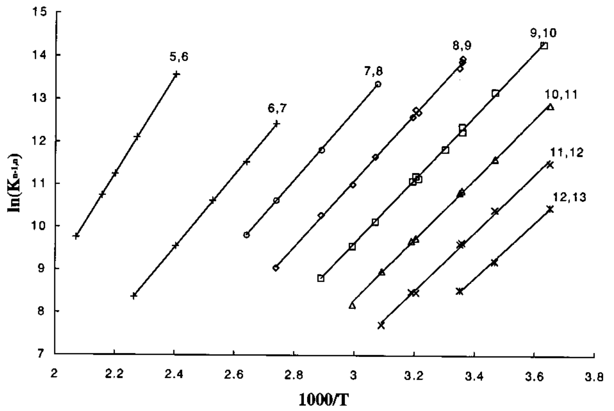

Figure 3. van't Hoff plots of hydration equilibria of Sr^{2+}: $Sr(H_2O)_{n-1}^{2+} + H_2O = Sr(H_2O)_n^{2+}$.

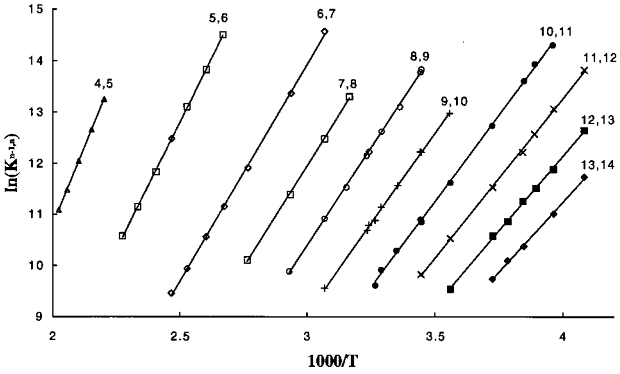

Figure 4. van't Hoff plots of hydration equilibria of Ba^{2+}: $Ba(H_2O)_{n-1} + H_2O = Ba(H_2O)_n^{2+}$.

TABLE 1: Thermochemical Data[a] for Reaction $M(H_2O)_n^{2+} = M(H_2O)_{n-1}^{2+} + H_2O$

Mg2+				Ca^{2+}			
n	Δ*G*	Δ*H*	Δ*S*	*n*	Δ*G*	Δ*H*	Δ*S*
6	16.0	24.6	29.1	6	16.1	25.3	31.1
7	12.8	20.3	25.3	7	10.9	16.9	20.2
8	10.9	18.0	23.8	8	9.6	16.1	21.9
9	9.5	17.0	25.1	9	8.4	15.3	23.1
10	8.1	15.7	25.5	10	7.3	14.5	24.0
11	7.0	14.3	24.3	11	6.5	13.3	22.7
12	6.2	12.9	22.3	12	5.8	13.0	24.1
13	5.6	12.3	22.5	13	5.2	12.4	24.4
14	5.1	12.1	23.7	14	4.7	11.9	24.2
Sr^{2+}				Ba^{2+}			
n	Δ*G*	Δ*H*	Δ*S*	*n*	Δ*G*	Δ*H*	Δ*S*
6	14.5	22.7	27.6	5	16.1	23.9	26.4
7	10.5	17.0	21.8	6	12.6	19.8	24.1
8	9.3	16.1	23.1	7	10.0	16.9	22.9
9	8.2	15.5	24.4	8	8.8	15.8	23.7
10	7.3	14.9	25.6	9	7.8	15.1	24.7
11	6.4	14.2	26.0	10	6.8	14.1	24.3
12	5.7	13.7	26.7	11	6.1	13.4	24.4
13	5.1	13.0	26.6	12	5.5	12.4	23.2
				13	5.0	11.6	22.4
				14	4.6	10.9	21.3

[a] Data from van't Hoff plots (Figures 1−4). Δ*G*° in kcal/mol at 298 K, standard state 1 atm. Δ*H*° in kcal/mol, Δ*S*° in cal/(K mol). Estimated error: Δ*G*°, 0.5 kcal/mol; Δ*H*°, 1 kcal/mol; Δ*S*°, 2 cal/(K mol).

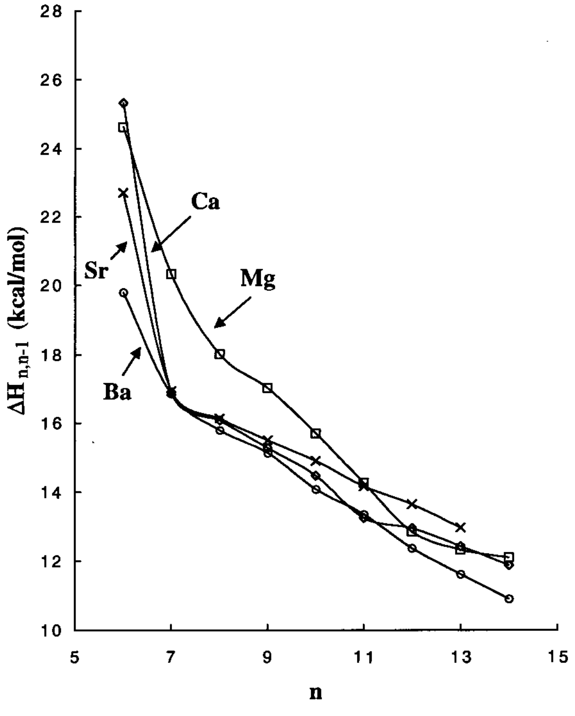

Figure 5. Enthalpy changes $\Delta H^\circ_{n,n-1}$ for reaction $M(H_2O)_n^{2+} = M(H_2O)_{n-1}^{2+} + H_2O$: (□) Mg; (◇) Ca; (×) Sr; (○) Ba.

data quoted in Table 1 are for the (n, $n-1$) reaction, which is the dehydration reaction rather than the opposite ($n-1$, n) hydration reaction, eq 1. The dehydration values for the enthalpies, free energies, and entropies are all positive, and the use of positive values facilitates the subsequent discussion.

(b) Binding Energies, Shell Structures, and Comparison with Theoretical Calculations. The sequential water dissociation enthalpies, $\Delta H^\circ_{n,n-1}$, for the hydrates of Mg^{2+}, Ca^{2+}, Sr^{2+}, and Ba^{2+}, Table 1, are shown plotted versus (n, $n-1$) in Figure 5, while Figures 6 and 7 provide the corresponding plots for the entropies $\Delta S^\circ_{n,n-1}$ and free energies $\Delta G^\circ_{n,n}-1$. The enthalpy plots for the four ions exhibit similarities and some significant differences. For all four ions the largest decrease of $\Delta H^\circ_{n,n-1}$ occurs between $\Delta H^\circ_{6,5}$ and $\Delta H^\circ_{7,6}$. For Ca^{2+} and Sr^{2+} this decrease is very large, while for Mg^{2+} and Ba^{2+} the decrease is considerably smaller. Thus, the differences $\Delta H_{6,5} - \Delta H_{7,6}$ are, in kcal/mol, 4.3 (Mg), 8.4 (Ca), 5.8 (Sr), and only 2.9 (Ba). The enthalpy values for the higher hydrates from $n = 7$ onward decrease much more slowly for all four ions, typically by less than 1 kcal/mol for Ca, Sr, Ba, while for Mg the decrease is somewhat faster and less regular. The observed behavior for Ca and Sr corresponds to expected changes when the inner coordination shell is completed at $n = 6$. The sixth water molecule is still strongly bonded, while the seventh and subsequent molecules go into an outer shell where the bonding is much weaker.

The ionic radii in angstroms are[24] $^{2+}$ 0.65 for Mg^{2+}, $^{2+}$ 0.94 for Ca^{2+}, $^{2+}$ 1.10 for Sr^{2+}, and $^{2+}$ 1.29 for Ba^{2+}. It is significant

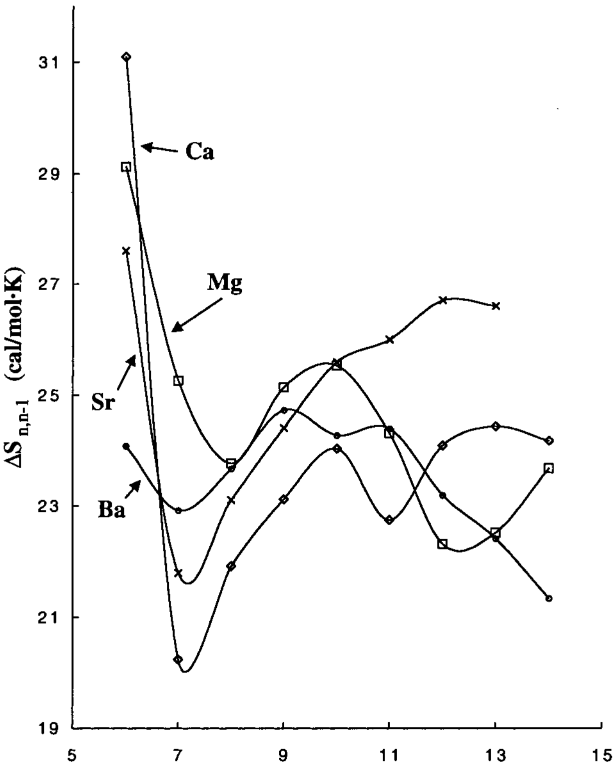

Figure 6. Entropy changes $\Delta S^\circ_{n,n-1}$ for reaction $M(H_2O)_n^{2+} = M(H_2O)_{n-1}^{2+} + H_2O$: (□) Mg; (◇) Ca; (×) Sr; (○) Ba.

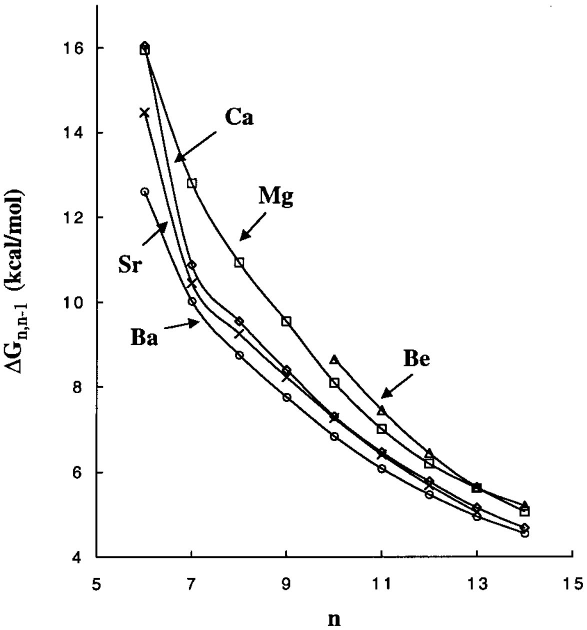

Figure 7. Free energy changes $\Delta G^\circ_{n,n-1}$ at $T = 298$ K for reaction $M(H_2O)_n^{2+} = M(H_2O)_{n-1}^{2+} + H_2O$: (□) Mg; (◇) Ca; (×) Sr; (○) Ba. The limited data obtained for beryllium (see Experimental Section) are also shown (△).

that $\Delta H^\circ_{6,5}(\mathrm{Ca}^{2+}) = 25.3$ kcal/mol is somewhat higher than $\Delta H^\circ_{6,5}(\mathrm{Mg}^{2+}) = 24.6$ kcal/mol. On the basis that the bonding of a water molecule in the first shell will be the stronger the smaller the ionic radius, one would have expected the reverse order. The low value for $\Delta H^\circ_{6,5}(\mathrm{Mg}^{2+})$ can be explained by assuming that for magnesium the inner six shell becomes "crowded" when it is completed by the introduction of the sixth molecule, an effect not present for the larger Ca^{2+}. One can invoke the changing size of the ions to explain also the very small change of 2.9 kcal/mol between $\Delta H_{6,5}$ and $\Delta H_{7,6}$ observed for Ba^{2+}. For this hugely bigger ion the six molecule inner shell is so uncrowded that it readily accepts seven and more molecules, and therefore, the sequential bond energy due to the seventh molecule is only slightly lower than that for the sixth.

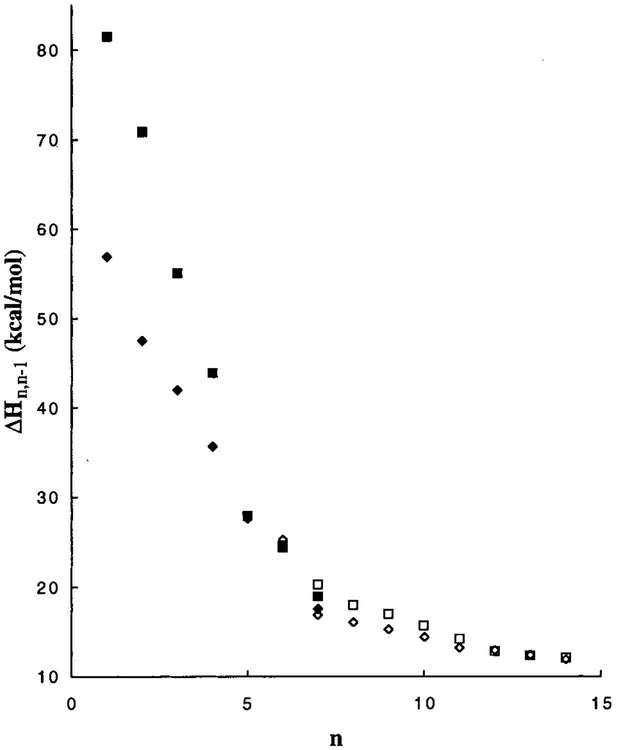

Figure 8. Enthalpy changes $\Delta H^\circ_{n,n-1}$ for Mg^{2+} and Ca^{2+}. Data are for $n = 1$ to $n = 7$. ■ (Mg) and ◆ (Ca) are theoretical results (Siegbahn and co-workers).[18] □ (Mg) and ◇ (Ca) from $n = 6$ to $n = 14$ are experimental results.

Theoretical results for the hydration of Mg^{2+} and Ca^{2+} obtained by Siegbahn and co-workers[18] for $n = 1$ to $n = 7$ prove very useful for the interpretation of the present experimental results. The theoretical energy changes for the lower hydrates are shown in Figure 8, together with the experimental $\Delta H^\circ_{n,n-1}$ changes from the present work. Numerical values for some of the computed hydration energies,[18] which are of special interest to the present discussion, are quoted in Table 2.

The agreement between the experimental and theoretical results is excellent (all values in kcal/mol):

$$\Delta H^\circ_{6,5}(\mathrm{Mg}^{2+}) = 24.6\ \text{(experimental)},\ 25.9\ \text{(theoretical)}$$

$$\Delta H^\circ_{6,5}(\mathrm{Ca}^{2+}) = 25.3\ \text{(experimental)},\ 25.5\ \text{(theoretical)}$$

$$\Delta H^\circ_{7,6}(\mathrm{Mg}^{2+}) = 20.3\ \text{(experimental)},\ 20.0\ \text{(theoretical)}$$

$$\Delta H^\circ_{7,6}(\mathrm{Ca}^{2+}) = 16.8\ \text{(experimental)},\ 19.0\ \text{(I)},\ 17.4\ \text{(II)}$$

The agreement is better than could be expected, since the experimental results are estimated to have an error of ±1 kcal/mol and the uncertainty in the theoretical results for such large hydrates is probably much higher, although since these are values for the successive hydration energies (n, $n-1$) and are obtained from differences of the total energies, $\Delta E_{n,0}$, cancellations of errors probably reduce significantly the theoretical uncertainties.

TABLE 2: Binding Energies of H_2O to Mg^{2+} and Ca^{2+} (from Theoretical Calculations by Siegbahn et al.[18])[a]

complex	$\Delta E^\circ_{n,0}$ (kcal/mol)	$(\Delta H^\circ_{n,0})^e$ (kcal/mol)	$(\Delta G^\circ_{n,0})^e$ (kcal/mol)	$(\Delta S^\circ_{n,0})^e$ (cal/(K mol))
$Mg(H_2O)_5$	279.4	285.9	236.6	165.4
$Mg(H_2O)_5(H_2O)^{2+\,b}$	300.2	307.8	248.2	199.6
$Mg(H_2O)_5(H_2O)^{2+\,c}$	299.0	306.8	246.5	202.1
$Mg(H_2O)_4(H_2O)_2{}^{2+\,c}$	299.5	307.5	246.9	203.4
$Mg(H_2O)_6{}^{2+}$	303.9	311.8	250.9	203.2
$Mg(H_2O)_6(H_2O)^{2+\,c}$	322.9	331.8	260.3	239.6
$Mg(H_2O)_7{}^{2+}$	307.8			
$Mg(H_2O)_6(H_2O)_2{}^{2+\,d}$	337.2	346.7	266.6	269.9
$Ca(H_2O)_5{}^{2+}$	209.7	215.2	168.5	156.7
$Ca(H_2O)_5(H_2O)^{2+\,c}$	228.2	234.8	177.9	190.7
$Ca(H_2O)_5(H_2O)^{2+\,c}$	228.5	235.4	177.4	194.6
$Ca(H_2O)_4(H_2O)_2{}^{2+\,c}$	225.7	233.0	174.0	198.0
$Ca(H_2O)_6{}^{2+}$	234.4	240.7	184.2	189.7
$Ca(H_2O)_6(H_2O)^{2+\,f}$	250.7	258.09	191.4	223.6
$Ca(H_2O)_6(H_2O)^{2+\,g}$	252.0	259.7	191.6	228.4
$Ca(H_2O)_7{}^{2+}$	248.2			

[a] Data quoted in Table 2 are only for $n = 5$ to $n = 8$ hydrates. A much wider set of energies are available in the original reference.[18] $\Delta E_{n,0}$ corresponds to the energy change at $T = 0$ K for the reaction $M(H_2O)_x(H_2O)_y{}^{2+} = M^{2+} + (x + y)H_2O$, where $x + y = n$. [b] Oxygen of outer-shell molecules forms one hydrogen bond to an inner-shell water molecule. [c] Oxygen of outer-shell molecule forms two hydrogen bonds, one each to hydrogens of two adjacent inner-shell water molecules. [d] Each outer water molecule forms two hydrogen bonds to different inner water molecules, and one inner water molecule is engaged in two hydrogen bonds. [e] Siegbahn et al.[18] published only the $\Delta E^\circ_{n,0}$ values at 0 K. The $\Delta H^\circ_{n,0}$, $\Delta G^\circ_{n,0}$, and $\Delta S^\circ_{n,0}$ values at $T = 298$ K given in the table were obtained from evaluated corrections to $\Delta E^\circ_{n,0}$ from the GAUSSIAN-94 file, graciously provided to us by the authors.[18] The vibrational frequencies were evaluated at the Hartree–Fock level.[18] [f] See structure **II** in text. [g] See structure **I** in text.

TABLE 3: Theoretical[18] Results for $Ca(H_2O)_6(H_2O^{2+})$

I	**II**
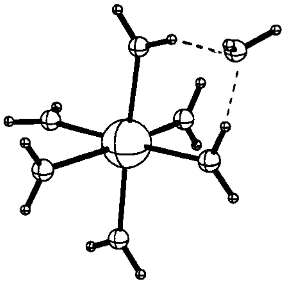	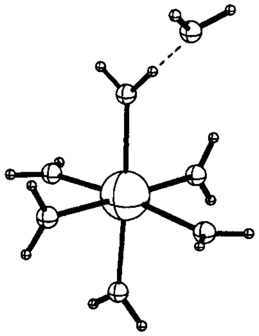
$\Delta H^\circ_{7,6} = 19.0$ kcal/mol	$\Delta H^\circ_{7,6} = 17.4$ kcal/mol
$\Delta S^\circ_{7,6} = 38.7$ cal/(K mol)	$\Delta S^\circ_{7,6} = 33.9$ cal/(K mol)
$\Delta G^\circ_{7,6}(298) = 7.4$ kcal/mol	$\Delta G^\circ_{7,6}(298) = 7.3$ kcal/mol
$\Delta G^\circ_{7,6}$ (380) = 4.2 kcal/mol	$\Delta G^\circ_{7,6}$ (380) = 4.5 kcal/mol

An exact correspondence between the theoretical and the experimental $\Delta H^\circ_{n,n-1}$ cannot be expected in certain special cases. The theoretical $\Delta H_{n,n-1}$ quoted above involve the n and $n - 1$ structures with the highest binding energies; see Table 2. However, in some cases two structures for a given n can be present that have binding enthalpies $\Delta H^\circ_{n,0}$ that differ by only 1 or 2 kcal/mol. This is the case for $n = 7$ of Ca^{2+} where there are two structures, $Ca(H_2O)_6(H_2O)^{2+}$ (**II**; see footnote b in Table 2) and $Ca(H_2O)_6(H_2O)^{2+}$ (**I**; see footnote c in Table 2), shown in Table 3.

The outer-shell water molecule can form two hydrogen bonds to two inner-shell molecules (see structure **I**), which leads to stronger bonding, $\Delta H_{7,6}$(**I**) = 19.0 kcal/mol, relative to the single hydrogen bond structure **II** where $\Delta H_{7,6}$(**II**) = 17.4 kcal/mol. However, the greater rotational freedom of the water molecules in **II** leads to a more favorable entropy so that the two structures have almost the same free energies at $T = 298$ and 380 K, the average temperature of the van't Hoff (7,6) plot (Figure 2). Therefore, very similar populations for the two structures can be expected at the experimental temperatures and the experimental $\Delta H^\circ_{7,6}$ should fall between the values for the two structures, $\Delta H_{7,6}$(**I**) = 19.0 kcal/mol and $\Delta H_{7,6}$(**II**) = 17.4 kcal/mol, presuming that these values are exact.

The theoretical values of $\Delta H^\circ_{n,n-1}$ ($n = 1$ to $n = 7$), Figure 8, are seen to decrease very rapidly, particularly so for Mg^{2+}. The decreases are largest at low n. Decreases of the sequential bond enthalpies are known to occur also for singly charged ions. Thus, experimental data[5,7] for Na^+ and K^+ exhibit such decreases. However, the decreases are relatively much smaller than is the case for the isoelectronic Mg^{2+} and Ca^{2+}. The decreases observed for the singly charged ions have been attributed[5,20] largely to repulsion between the permanent and induced dipoles of the ligands and to Pauli repulsion. Ion core polarization effects[25] and to a lesser extent charge transfer from the ligands to the core ion whose importance increases for small ions such as Li^+ are also involved.[5,25] For the doubly charged ions such as Mg^{2+} and Ca^{2+} the same factors will be involved also. Since the doubly charged ions are much smaller than the isoelectronic Na^+ and K^+, the dipole and Pauli repulsions between the ligands will be bigger. Increased charge transfer is also expected and will lead to larger bond energy decreases. Siegbahn et al.[18] point out that the charge transfer from the water ligands to the s and p orbitals of the doubly charged ions is a much more important effect than is the case for the singly charged ions and by far the dominant effect for small ions such as Be^{2+} and Mg^{2+}.

The decrease of the binding energies from $n = 1$ onward is not completely regular, and this is particularly so for Mg^{2+} where larger decreases are observed after $n = 2$ and after $n = 4$ (Figure 8). These probably indicate the relative ability of the specific $M(H_2O)_n{}^{2+}$ geometries to minimize the ligand repulsions: $n = 2$ (linear), good; $n = 3$ (trigonal planar), not so good; $n = 4$ (tetrahedral), good; etc. The sequential bonding for Mg^{2+} decreases much more quickly so that $\Delta H_{5,4}(Mg^{2+})$ becomes essentially the same as $\Delta H_{5,4}(Ca^{2+})$. The more rapid decrease for Mg^{2+} should be mostly due to the more extensive electron transfer from the ligand to the core ion, expected for the much smaller Mg^{2+} ion. However, crowding of the inner shell at $n = 5$ should be involved also.

The theoretical results predict that the inner shell is complete at $n = 6$ for both Mg^{2+} and Ca^{2+}. Thus, for $n = 7$, for the first time the bonding in the symmetrical structure $M(H_2O)_7{}^{2+}$ is weaker than that for the inner–outer shell structure $M(H_2O)_6(H_2O)^{2+}$ for both Mg^{2+} and Ca^{2+} (see Table 2).

An examination of the theoretical binding enthalpies for the $n = 6$ isomeric structures, $M(H_2O)_4(H_2O)_2{}^{2+}$, $M(H_2O)_5(H_2O)^{2+}$, and $M(H_2O)_6{}^{2+}$ (Table 2), is very instructive. For Mg^{2+} the less stable isomers $M(H_2O)_4(H_2O)_2{}^{+}$ and $M(H_2O)_5(H_2O)^{2+}$ are only ~4 kcal/mol less stable than the $M(H_2O)_6{}^{2+}$ species, while for Ca^{2+} the corresponding stability difference of ~6 kcal/mol is considerably bigger. The relatively greater stability of the above inner–outer shell isomers for Mg^{2+} relative to that for Ca^{2+} is another indication of the rapidly increasing ligand repulsion for Mg^{2+}, which causes the six molecule inner shell for Mg^{2+} to be relatively more crowded.

As previously mentioned, the experimental $\Delta H^\circ_{n,n-1}(Mg^{2+})$ values for $n > 6$ become larger than the corresponding values for Ca^{2+} (see Figure 5). This change can be understood. Since for both Mg^{2+} and Ca^{2+} outer-shell molecules are involved at $n > 6$, crowding of the outer shell is not present and the bonding for the Mg^{2+} hydrate is stronger, since the inner shell for Mg^{2+} is smaller. Furthermore, the hydrogens of the inner-shell molecules of the Mg ion have a more protic character due to the more extensive charge transfer to the Mg ion, and this increased protic character will lead to stronger hydrogen bonds between the inner- and outer-shell water molecules. As the second shell of Mg^{2+} starts filling up, these advantages over Ca^{2+} will become smaller and the $\Delta H^\circ_{n,n-1}$ values for the two ions should get closer, as is observed (Figure 5).

The very small change between the experimental $\Delta H_{6,5}$ and $\Delta H_{7,6}$ for Ba^{2+} was attributed in the prior discussion to Ba^{2+} being so big that it can readily accommodate more than six molecules in its inner shell. This conclusion is indirectly supported by the theoretical calculations[18] (Table 2). The binding energies $\Delta E_{n,0}$ for $Ca(H_2O)_6(H_2O)^{2+} = 252$ kcal/mol and ${Ca(H_2O)_7}^{2+} = 248$ kcal/mol differ by only 4 kcal/mol. One might expect that the ${M(H_2O)_7}^{2+}$ isomer relative to the $M(H_2O)_6(H_2O)^{2+}$ isomer may become equally or more stable for Sr^{2+} and definitely more stable for Ba^{2+}. Thus, the observed differences in the $\Delta H^\circ_{n,n-1}$ values in this range of n, between Ca^{2+} and Sr^{2+} (Figure 5), is almost certainly due to participation of the ${M(H_2O)_7}^{+}$ structure for Sr^{2+}. Ba^{2+} accommodates seven water molecules in the inner shell even better, and the difference between the bond enthalpies for $n = 6$ and $n = 7$ should be smaller than that for Sr^{2+}, in agreement with the experimental results (Figure 5). Probably eight and more molecules may also fit in the inner shell of Ba^{2+}. The values of $\Delta H^\circ_{n,n-1}$ in the region $n = 7$ to $n = 9$ for Ba^{2+} are very close to those for the smaller ions. The ability of Ba^{2+} to compete with the smaller ions in this region of n may be due to inner-shell bonding for Ba, while for the smaller ions the bonding occurs from an outer shell. For $n > 9$ the $\Delta H^\circ_{n,n-1}$ for Ba^{2+} becomes smaller than those for the other ions, and this changeover may indicate a shift to an outer shell at this n.

(c) Sequential Entropy Changes. $\Delta S^\circ_{n,n-1}$ and Structural Information. The experimental entropy changes $\Delta S^\circ_{n,n-1}$ for the doubly charged Mg, Ca, Sr, and Ba are given in Table 1 and are shown plotted vs n in Figure 6. The shapes of the $\Delta S^\circ_{n,n-1}$ curves are somewhat similar for Mg^{2+}, Ca^{2+}, and Sr^{2+}. The entropy change $\Delta S^\circ_{6,5}$ is by far the biggest, and $\Delta S^\circ_{7,6}$ is the smallest for Ca^{2+} and Sr^{2+}, while for Mg^{2+} it is the second smallest. The initial dip between $\Delta S^\circ_{6,5}$ and $\Delta S^\circ_{7,6}$ is followed by an increase that flattens out at $n \approx 13$ for Ca^{2+} and Sr^{2+}, while Mg^{2+} shows a more complicated behavior. The Ba^{2+} ion is distinguished by relatively very small changes with n.

We shall examine first the entropy changes for Ca^{2+}, which are quite regular and may be expected to be the simplest to interpret. As discussed in the previous section, for enthalpies, Ca^{2+} exhibits the most distinct transition between an inner shell with $n = 6$ molecules and an outer shell for the seventh and higher n molecules. By this we mean that the (7, 6) equilibrium involves almost exclusively the structures $Ca(H_2O)_6(H_2O)^{2+}$ and ${Ca(H_2O)_6}^{2+}$, while for Mg, Sr, and Ba other shell structures, such as ${M(H_2O)_7}^{2+}$ (M = Sr, Ba), $M(H_2O)_5{(H_2O)_2}^{2+}$, and $M(H_2O)_5(H_2O)$ (M = Mg), may be also present at the (7, 6) equilibrium. For Ca^{2+}, a qualitative account of the observed entropies in the transition region and somewhat beyond it can be given as follows. The translational energy changes $\Delta S^\circ_{n,n-1}$(trans), evaluated with the Sackur−Tetrode equation, turn out to be essentially the same for all four ions and all n when $n \geq 6$. This comes about because at high n, the mass values of the reactant $M(H_2O)_n$ and product $M(H_2O)_{n-1}$ are very close and cancel approximately, while the mass of the product H_2O is always the same (see Table 4). By subtraction of $\Delta S_{n,n-1}$(trans) from the experimental values of $\Delta S^\circ_{n,n-1}$(exp), one obtains values for the combined rotational and vibrational changes $\Delta S_{n,n-1}$(rot,vib); see Table 4. The values obtained are negative even though in the dissociation of water from the hydrate, two (loose) vibrations and one internal rotation are replaced by three external rotations of the freed water molecule, and this particular change is associated with a positive entropy. The negative $\Delta S^\circ_{\text{rot,vib}}$ (Table 4) should be due to increases in the vibrational frequencies in the $(n - 1)$ product ion due to the increased bonding of the $(n - 1)$ ligands to the core ion. A negative $\Delta S^\circ_{n,n-1}$(rot,vib) is also observed for the singly charged ions, such as Na^+ and K^+ ions (see Table 4), and the same explanation should hold also for these species.

TABLE 4: Entropy $\Delta S^\circ_{n,n-1}$ Contributions[a]

	${Ca_{(6,5)}}^{2+}$	${Ca_{(7,6)}}^{2+}$	${Ca_{(8,7)}}^{2+}$	${Na_{6,5}}^{+}$	${K_{6,5}}^{+}$
ΔS°(exp)	31.1 (33.0)[d]	20.2 (38.7)[e] (33.9)[f]	21.9	26.0[g]	25.7[g]
ΔS°(trans)[b]	34.2	34.3	34.3	34.1	35.1
ΔS°(rot,vib)[c]	−3.1	−14.1	−12.4	−8.1	−10.6

[a] All values in cal/(Kdegree mol) at 298 K. [b] Translational entropy evaluated with Sackur−Tetrode equation $\Delta S^\circ_{\text{trans}} = 1.5R \ln(m_{n-1}m_{H_2O}/m_n) + 2.5R \ln T - 2.311$, where m stands for molar mass in daltons. [c] Entropy change due to rotational and vibrational changes. [d] Theoretical result based on data in Table 2. [e] Theoretical result for structure **I** of $Ca(H_2O)_6(H_2O)^{2+}$. [f] Theoretical result for structure **II** of $Ca(H_2O)_6(H_2O)^{2+}$. [g] Experimental determinations.[5]

Concerning the Ca^{2+} data, the question must be asked: Why is there such a large difference between $\Delta S^\circ_{6,5}(\text{rot,vib}) = -3.1$ relative to $\Delta S_{7,6}(\text{rot,vib}) = -14.1$ and $\Delta S^\circ_{8,7}(\text{rot,vib}) = -12.4$ (Table 4)? One can expect that the bond-strengthening process and the increase of the frequencies should be at least as large if not larger for the inner-shell process (6, 5) relative to the (7, 6) and (8, 7) where an outer molecule is leaving. Theoretical results for $\Delta S^\circ_{7,6}$ and $\Delta S^\circ_{6,5}$ of Ca^{2+} are available (Tables 2 and 4). The theoretical value for $\Delta S^\circ_{6,5} = 32.8$ is close to the experimental value of 31.1 (all values in cal/(K mol)). However, there is a big disagreement for $\Delta S^\circ_{7,6}$ where the theoretical values are 38.7 when structure **I** is used for $Ca(H_2O)_6(H_2O)^{2+}$, while for structure **II**, the value is 33.9. Both values are very much higher than the experimental result of 20.2. We are essentially certain that the experimental result is the correct value, and therefore, the question arises: What phenomena are not properly accounted for by the theoretical results? A tentative explanation is given below.

As discussed in the previous section, owing to the opposing effects of the enthalpy and entropy changes, structures **I** and **II** have almost the same free energies (see data provided with structures **I** and **II**), and therefore, one expects rougly equal populations of both structures at the temperatures of the experimental measurements. Examination of structures **I** and **II** indicates that the conversion from **I** to **II** and vice versa will be very facile because it requires only partial rotations of one of the neighboring inner H_2O ligands and very small motions of the outer-shell H_2O molecule. The activation free energy for the conversion is expected to be very small (1 or 2 kcal/mol), and this will allow the outer molecule to rapidly travel to different sites of the outer shell. This means that a much larger space will be available through which the molecule can travel in a quasi translational mode. This freedom will lead to a much higher entropy for the $Ca(H_2O)_6(H_2O)^{2+}$ ion and thus to a specially low value for $\Delta S^\circ_{7,6}$, as observed experimentally.

A very rough (upper limit) estimate of the entropy increase due to such a quasi translational mode can be made by assuming that the outer-shell molecule undergoes free translation on the surface of a sphere with radius $R = 4.5$ Å. This radius corresponds to the calculated[18] distance between the ion and the oxygen of the outer-shell molecule. Replacing this surface with a flat, square surface of the same area and using the energy levels for a free particle in a two-dimensional box, one can numerically evaluate the partition function Q and from it obtain the entropy. The value, at 298 K, is $S^\circ_{\mathrm{trans}} = 18.66$ cal/(K mol). This value is essentially identical to the value $\Delta S^\circ_{\mathrm{trans}} = 18.75$ cal/(K mol) obtained with the partition function equation $Q = (2\pi mkT/h^2)4\pi R^2$, valid for macroscopic two-dimensional boxes. Since the translational motion replaces two bending vibrations in the "rigid" structures **I** and **II** of $\mathrm{Ca(H_2O)_6H_2O^{2+}}$ and since each of these is expected to be associated with an entropy of 1 to 2 cal/(K mol), a difference of $\Delta S^\circ \approx 15$ cal/(K mol) is predicted between the entropy of the state with a quasi translating molecule and those of the more rigid states corresponding to structures **I** and **II**. This value is very close to the difference between the experimental $\Delta S^\circ_{7,6}$ and the theoretical values for structures **I** and **II** (see Table 4).

For the higher hydrates $n = 8$, 9, etc., the situation should be similar, but the available sites will be decreasing and the $\Delta S^\circ_{n,n-1}$ values would gradually increase above the minimum value observed for $\Delta S^\circ_{7,6}$. The relatively low value for $\Delta S^\circ_{11,10}$ (Figure 6), which is out of line, may be due to an experimental error or may be real and indicate a true effect, which we will not attempt to explain.

The entropy change curve for Sr is very similar to that of Ca (Figure 6). The (6, 5) value is considerably smaller than that for Ca. Probably this reflects the weaker bonding and the relative greater freedom of the six water molecules in $\mathrm{Sr(H_2O)_6^{2+}}$, owing to the larger radius of Sr. The entropy change (7, 6) is larger than that for Ca, and that may be due to participation of $\mathrm{Sr(H_2O)_6(H_2O)^{2+}}$ and $\mathrm{Sr(H_2O)_7^{2+}}$ in the seven hydrate (see discussion of ΔH values, section b). A larger $\Delta S_{7,6}$ is expected for $\mathrm{Sr(H_2O)_7^{2+}}$ because this structure is expected to be tight, i.e., of entropy lower than that of the loose $\mathrm{Sr(H_2O)_6(H_2O)^{2+}}$ species. Larger than $n = 7$ inner-shell structures are probably not important for strontium, and therefore, the $\Delta S^\circ_{n,n-1}$ values for this ion above $n = 7$ show a regular increase as observed and rationalized for $\mathrm{Ca^{2+}}$.

For $\mathrm{Ba^{2+}}$ the $\Delta S^\circ_{n,n-1}$ values change little for $n = 6$ to $n = 11$. Inner-shell structures $\mathrm{Ba(H_2O)}_n{}^{2+}$ are expected to be competitive or even more stable than inner-outer shell species $\mathrm{Ba(H_2O)}_k\mathrm{(H_2O)}_{n-k}{}^{2+}$, for $n = 7$ to $n \approx 10$ (see preceding section). Since the bonding in both of these is relatively weak compared with that for the smaller ions, relatively small values for $\Delta S^\circ_{n,n-1}$ and relatively small changes with n can be expected in this range, in agreement with the experimental observations (Figure 6).

The entropy changes for $\mathrm{Mg^{2+}}$ (Figure 6) leading to a curve with two minima are the most complex. $\Delta S^\circ_{6,5}$ is smaller for Mg relative to Ca. This could be due to the poorer bonding in the crowded $\mathrm{Mg(H_2O)_6^{2+}}$ and the possible participation of the loose $\mathrm{Mg(H_2O)_5(H_2O)^{2+}}$ structures.

The maximum in the ΔS curve for $n = 10$ (Figure 6) most likely is not an experimental artifact. A second set of experimental measurements from $n = 8$ to $n = 12$ (see Experimental Section) led to close agreement with the first set of results. We can only speculate about the physical origin of this entropy change feature. Theoretical calculations, performed in this work at the B3LYP/6-311++G** level, predict that the 10-molecule hydrate $\mathrm{Mg(H_2O)_6(H_2O)_4^{2+}}$ of structure **III**, where each outer molecule forms two hydrogen bonds, is more stable by 5.4 kcal/mol than the hydrate of structure **IV** where only single hydrogen bonds are involved. It is possible that **III** is present at significant concentration in the $n = 10$ population of the *magnesium* hydrates.

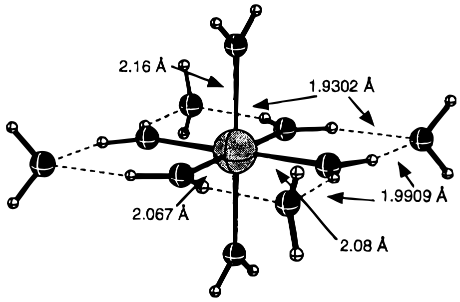

Structure III

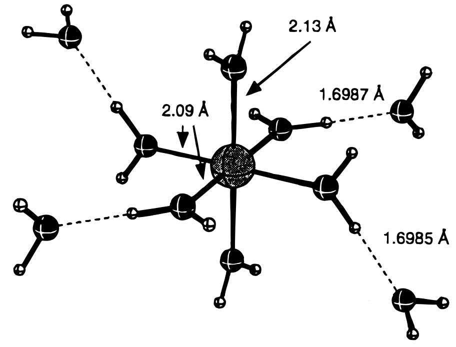

Structure IV

Dissociation of one water molecule out of structure **III** may be expected to lead to a high $\Delta S_{10,9}{}^{2+}$ because two hydrogen bonds are broken and the high symmetry of **III** is not present in the $n = 9$ hydrate. This explanation also makes the implicit assumption that for $n = 10$, structure **III** and the structures of neighboring n of magnesium are relatively strongly bonded so that the quasi translational motion assumed above for Ca at $n = 7$ and somewhat higher n is not present in Mg.

(d) Relationship of Gas-Phase Bond Energies to Total Energies of Solvation in Liquid Water. The $\Delta H_{n,n-1}$ enthalpy plot, Figure 6, indicates that for high n, the $\Delta H_{n,n-1}$ values for $\mathrm{Mg^{2+}}$ and $\mathrm{Ca^{2+}}$ become nearly equal. Assuming that this is approximately true also for values of n beyond the present measurements, estimates for the differences between the total energies of solvation in liquid water, $\Delta H^\circ_{\mathrm{h}}$, between $\mathrm{Mg^{2+}}$ and $\mathrm{Ca^{2+}}$, can be obtained from the differences of the sum of the sequential energies equal to $\Delta H^\circ_{0,n}$. The highest n for which data are available is $n = 14$, and we obtain $\Delta H_{0,n}$ by using theoretical values[18] for $\Delta H^\circ_{0,6}$ (see Table 2 and the $\Delta H^\circ_{6,14}$ from the experimental results). This leads to

$$\Delta H^\circ_{0,14} = \Delta H^\circ_{0,6} + \Delta H^\circ_{6,14}$$

$$\Delta H^\circ_{0,14}(\mathrm{Mg^{2+}}) = -311.8 + (-123.1) = -434.9\ \mathrm{kcal/mol}$$

$$\Delta H^\circ_{0,14}(\mathrm{Ca^{2+}}) = -240.7 + (-113.3) = -354.0\ \mathrm{kcal/mol}$$

$$\Delta H_{0,14}(\mathrm{Mg^{2+}}) - \Delta H_{0,14}(\mathrm{Ca^{2+}}) = -81.0\ \mathrm{kcal/mol}$$

$$\Delta H_{\mathrm{h}}(\mathrm{Mg^{2+}}) - \Delta H_{\mathrm{h}}(\mathrm{Ca^{2+}}) = 462 - (-379) = -83.0\ \mathrm{kcal/mol}^{26}$$

The difference, which leads to −81 kcal/mol, can be compared with the difference for the total hydration energies, ΔH_{h}, in liquid water of −83 kcal/mol, shown above. The ΔH_h were taken from Marcus.[26] The close agreement may be fortuitous to a certain extent. Nevertheless, the data show that relative ΔH_h for different doubly charged ions can be predicted within a few kcal/mol from accessible gas-phase hydration energies. An analogous calculation for the free energies leads to $\Delta G^\circ_{0,14}(\mathrm{Mg}^{2+}) - \Delta G^\circ_{0,14}(\mathrm{Ca}^{2+}) = -74.0$ kcal/mol, which can be compared with $\Delta G^\circ_h(\mathrm{Mg}^{2+}) - \Delta G^\circ_h(\mathrm{Ca}^{2+}) = -77.3$ kcal/mol.[26]

The theoretical calculations[18,19,22] and the present thermochemical measurements provide a very good account of the hydration of the biologically important Mg^{2+} and Ca^{2+} ions. However, these are only very preliminary steps concerning the coordination of these ions in biological systems, where the coordinating oxygens are often due to peptide carbonyl groups or specific peptide residues. Equilibrium determinations presently underway in this laboratory with acetone instead of water indicate very large differences between water and acetone. Thus, the interactions with acetone at low n ($n = 1, 2, 3$) are very much stronger. But they fall off much more quickly as n is increased so that the $\Delta H_{6,5}$ and $\Delta H_{7,6}$ for acetone are lower than those for water. This effect should be due to the larger extent of charge transfer from the carbonyl oxygen to the core ion. Transitions to the outer shell occur later than those for water, leading to seven or even eight coordination as is observed for calcium sites in proteins.[27,28] The delayed transitions to the outer shell are expected because of the absence of strong hydrogen bonding between the inner and outer shell. We are quite confident that extension of the measurement to other model molecules such as *N*-methylacetamide and ligands corresponding closely to the residues of amino acids often involved in Ca^{2+} and Mg^{2+} complexation will provide useful insights into the coordination and bonding of biocomplexes such as metalloenzymes.

Acknowledgment. The authors are very grateful to Drs. M. Pavlov, P. Siegbahn, and M. Sandström for providing them with the GAUSSIAN-94 files of their calculations, which contained the theoretical evaluations of the enthalpy and free energy changes. This work was supported by grants from the Natural Sciences and Engineering Research Council (NSERC) of Canada.

References and Notes

(1) Hogg, A. M.; Kebarle, P. *J. Chem. Phys.* **1965**, *43*, 449.

(2) Kebarle, P.; Searles, S. K.; Zolla, A.; Scarborough, J.; Azshadi, M. *J. Am. Chem. Soc.* **1967**, *25*, 915.

(3) Hogg, A. M.; Haynes, R. N.; Kebarle, P. *J. Am. Chem. Soc.* **1966**, *88*, 28.

(4) Searles, S. K.; Kebarle, P. *J. Phys. Chem.* **1968**, *72*, 742.

(5) Dzidic, I.; Kebarle, P. *J. Phys. Chem.* **1970**, *74*, 1966.

(6) Kebarle, P. *Annu. Rev. Phys. Chem.* **1977**, *28*, 445.

(7) Keesee, R. G.; Castleman, A. W. *J. Phys. Chem. Ref. Data* **1986**, *15*, 1011.

(8) Kebarle, P. *Modern Aspects of Electrochemistry*; Conway, B. E., Bockris, J. O'M., Eds.; Plenum Press: New York, 1974; Vol. 9, p 1.

(9) Marcus, Y. *Ion Solvation*; Wiley-Interscience: Chichester, 1985; Chapter 2, p 13.

(10) (a) Kraemer, W. P.; Diercksen, G. H. F. *Chem. Phys. Lett.* **1970**, *5*, 463. (b) Diercksen, G. H. F.; Kraemer, W. P. *Theor. Chim. Acta* **1972**, 387. (c) Kishenmacher, H.; Popkie, H.; Clementi, E. *J. Chem. Phys.* **1973**, *59*, 5842.

(11) Chandrasekhar, J.; Spellmeyer, D. C.; Jorgensen, W. L. *J. Am. Chem. Soc.* **1984**, *106*, 903.

(12) Okamura, M.; Yeh, L. I.; Lee, Y. T. *J. Chem. Phys.* **1988**, *88*, 79.

(13) Spears, K. G.; Fehsenfeld, F. C. *J. Chem. Phys.* **1972**, *565*, 5698.

(14) (a) Yamashita, M.; Fenn, J. B. *J. Phys. Chem.* **1984**, *88*, 4451, 4671. (b) Whitehouse, C. M.; Dreyer, R. N.; Yamashita, M.; Fenn, J. B. *Anal. Chem.* **1985**, *57*, 675.

(15) (a) Blades, A. T.; Jayaweera, P.; Ikonomou, M. G.; Kebarle, P. *J. Chem. Phys.* **1990**, *92*, 5900. (b) *Int. J. Mass Spectrom. Ion Processes* **1990**, *101*, 325; **1990**, *102*, 251.

(16) (a) Blades, A. T.; Klassen, J. S.; Kebarle, P. *J. Am. Chem. Soc.* **1996**, *118*, 12437. (b) Ikonomou, M. G.; Blades, A. T.; Kebarle, P. *J. Am. Soc. Mass Spectrom.* **1991**, *2*, 497.

(17) Klobukowski, M. *Can. J. Chem.* **1992**, *70*, 589.

(18) Pavlov, M.; Siegbahn, P. E. M.; Sandström, M. *J. Phys. Chem. A* **1998**, *102*, 219.

(19) Bock, C. W.; Katz, A. K.; Glusker, J. *J. Am. Chem. Soc.* **1995**, *117*, 3754.

(20) Katz, A. K.; Glusker, J. P.; Beebe, S. A.; Bock, C. W. *J. Am. Chem. Soc.* **1996**, *118*, 5752.

(21) Carugo, O.; Djinovic, K.; Rizzi, M. *J. Chem. Soc., Dalton Trans.* **1993**, 2127.

(22) (a) Bock, C. W.; Glusker, J. *Inorg. Chem.* **1993**, *32*, 1242. (b) Bock, C. W.; Glusker, J. *Inorg. Chem.* **1994**, *33*, 419.

(23) Markham, G. D.; Glusker, J. P.; Bock, C. L.; Trachtman, M.; Bock, C. W. *J. Phys. Chem.* **1996**, *100*, 3488.

(24) Cotton, A. F.; Wilkinson, G. *Advanced Inorganic Chemistry*; Interscience Publishers: New York, 1966.

(25) (a) Bauschlicher, C. W., Jr.; Langhoff, S. R.; Partridge, H.; Rice, J. E.; Komornicki, A. *J. Chem. Phys.* **1991**, *95*, 5142. (b) Bauschlicher, C. W., Jr.; Langhoff, S. R.; Partridge, H. *J. Chem. Phys.* **1991**, *94*, 2068. (c) Bauschlicher, C. W., Jr.; Sodupe, M.; Partridge, H. *J. Chem. Phys.* **1992**, *96*, 4453.

(26) Marcus, Y. *Ion Solvation*; John Wiley and Sons: Chichester, 1985; p 107.

(27) Weis, W. I.; Drickamer, K.; Hendrickson, W. A. *Nature* **1992**, *360*, 127.

(28) Kretsinger, R. H. *Annu. Rev. Biochem.* **1976**, *45*, 239.